

ChemComm

Accepted Manuscript



This is an *Accepted Manuscript*, which has been through the Royal Society of Chemistry peer review process and has been accepted for publication.

Accepted Manuscripts are published online shortly after acceptance, before technical editing, formatting and proof reading. Using this free service, authors can make their results available to the community, in citable form, before we publish the edited article. We will replace this *Accepted Manuscript* with the edited and formatted *Advance Article* as soon as it is available.

You can find more information about *Accepted Manuscripts* in the [Information for Authors](#).

Please note that technical editing may introduce minor changes to the text and/or graphics, which may alter content. The journal's standard [Terms & Conditions](#) and the [Ethical guidelines](#) still apply. In no event shall the Royal Society of Chemistry be held responsible for any errors or omissions in this *Accepted Manuscript* or any consequences arising from the use of any information it contains.

Cite this: DOI: 10.1039/c0xx00000x

www.rsc.org/chemcomm

Communication

A photofuel cell comprising titanium oxide and silver(I/O) photocatalysts for use of acidic water as a fuel[‡]Yuta Ogura,^a Seiji Okamoto,^a Takaomi Itoi,^b Yukiko Fujishima,^{c,a} Yusuke Yoshida,^a and Yasuo Izumi^{a*}

Received (in XXX, XXX) Xth XXXXXXXXXX 20XX, Accepted Xth XXXXXXXXXX 20XX

DOI: 10.1039/b000000x

A photofuel cell comprising two photocatalysts of TiO₂ and Ag-TiO₂ is demonstrated. The open circuit voltage, short circuit current, and maximum electric power of the PFC were 1.59 V, 74 μA, and 14 μW, respectively. The electron flow was rectified due to the Schottky barrier between TiO₂ and Ag nanoparticles.

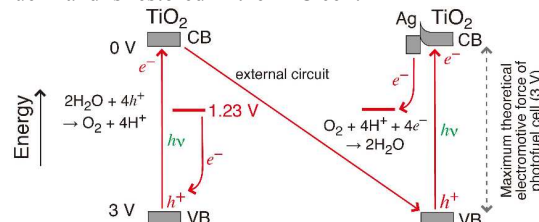
Fossil fuels have been utilized as the essential energy source for industrialization. The industrial CO₂ emissions have led to increase in the level of atmospheric CO₂ concentration (400 ppm), and the effects of this increase to global warming cannot be underestimated. The development of renewable energy as a replacement for fossil fuels has been slow.^{1,2} Among the renewable energies, solar energy has the greatest potential. Although silicon solar cell (Si SC) has been commercialized, the technology that can convert solar energy to electricity often needs subsidies to spread more widely.³ Other types of SCs,⁴ and fuel cells (FCs) that use hydrogen fuel⁵ potentially obtained using solar energy⁶ have been extensively investigated. However, all the requisites (sustainability, durability, and an electromotive force of 1–3 V per cell) have not been fully satisfied.

In this study, we demonstrate a new device: a photofuel cell (PFC) utilizing two photocatalysts of TiO₂ and silver(0/I)-doped TiO₂ on an electrode film, both immersed in acidic solutions separated by a proton-conducting polymer (PCP). The cell mechanism of redox reactions over the photocatalysts and the flow of electrons and protons in the cell facilitates a theoretical electromotive force of 3 V if some reasons (charge recombination in electrodes, electrons confined in Ag, and reverse electron flow from cathode to anode) for overvoltage are not taken into account. Moreover, the use of acidic water as a fuel is inexpensive and sustainable.

The concept of PFC is shown in Scheme 1. The band gap values for anatase- and rutile-type TiO₂ are 3.2 and 3.0 eV,^{7,8} respectively, and charges (holes, electrons) are separated by UV (and minor visible) light irradiation. The holes in TiO₂ diffused to the surface to photooxidize water, while the electrons in Ag-TiO₂ diffused to the TiO₂ surface and then to Ag nanoparticles to photoreduce O₂ molecules. Thus, in the cell, electron flow from conduction band (CB) of TiO₂ to the valence band (VB) of Ag-TiO₂ is obtained. Because the Schottky barrier is formed at the interface between TiO₂ and Ag nanoparticles, the electron flow from TiO₂ to Ag is rectified.

This concept of PFC comprising two photoelectrodes is

different from FCs comprising a photoanode and conventional cathode such as Pt-carbon,^{9–15} dye-sensitized SC comprising dye on a semiconductor and conventional cathode,³ and combination of two photocatalysts separated by PCP film to produce O₂ and H₂ independently from water.^{16–18} Recently, a PFC comprising WO₃ photoanode and a Cu₂O/Cu photocathode was reported using organic dyes as fuel.¹⁹ In this study, (acidic) water is used as a fuel¹⁵ and is restored in the PFC cell.



Scheme 1. The energy diagram of PFC comprising two photocatalyst electrodes.

An Ag-supported TiO₂ (Ag-TiO₂) sample was calcined at 673 K. The color was light yellow, which indicated the presence of metallic Ag.²⁰ However, the color changed to purple under air after 24 h (Fig. 1A). Silver K-edge extended X-ray absorption fine structure (EXAFS, Fig. 1B-a) demonstrated the dominance of Ag₂O based on the interatomic pair of Ag and O at 0.2305 nm by curve-fit analysis (Table S1a). Scanning electron microscopy (SEM, Fig. 2A), transmission electron microscopy (TEM, Fig. 2B) and high-resolution (HR) TEM (Fig. 2D) revealed Ag₂O nanoparticles of mean 3.8 nm accompanying lattice intervals between 0.222 and 0.249 nm, corresponding to (002) lattice ($a/2 = 0.2361$ nm) and not (111) lattice ($a/\sqrt{3} = 0.2726$ nm).²¹ The brightness of the high angle annular dark field (HAADF)-scanning TEM (STEM) image was proportional to the square of atomic weight and distinguished ⁴⁷Ag and ²²Ti atoms (Figs. 2C, 2E). Indeed, the distribution of Ag₂O nanoparticles on TiO₂ was clearly observed (Fig. 2C), and the atomic resolution image of a single Ag₂O nanoparticle supported the presence of Ag₂O (Fig. 2E), as shown in HR-TEM image (Fig. 2D). A weak peak due to the interatomic pair of Ag and Ag because of metallic Ag⁰ was also observed by EXAFS (Fig. 1B-a2); however, the population was small (~10% on atom basis) based on the curve-fit analysis (Table S1a).

The photocurrent generation of PFC comprising TiO₂ and Ag-TiO₂, both placed on an indium tin oxide (ITO)-coated Pyrex glass electrode, was tested under N₂ and O₂ gas flows,

respectively, separated by a PCP film. When the Ag-TiO₂ film on electrode was immersed in a HCl solution with a pH of 2.0, the color of film changed to light yellow within 5 s (Fig. 1A, Right). The interatomic pair distance between Ag and Cl at 0.262 nm

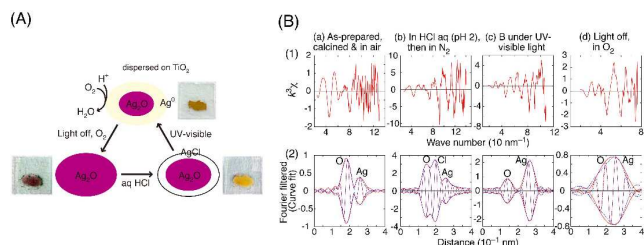


Fig. 1. (A) Transformation of Ag active sites on Ag-TiO₂ photocatalyst. (B) (a) Silver K-edge EXAFS spectra for as-prepared Ag-TiO₂ (3.0 wt%-Ag), (b) sample a was immersed in HCl solution of pH 2.0 and then kept under 101 kPa of N₂, (c) sample b was irradiated under UV-visible light, and (d) light was turned off and sample c was kept under 101 kPa of O₂. Note that (1) corresponds to the k^3 -weighted EXAFS χ -function and (2) corresponds to best-fit results in R -space to the Fourier-filtered transformed data. The red line represents the experimental values, and the blue line represents calculated values. The solid line represents the magnitude and the dotted line represents the imaginary part in panel (2).

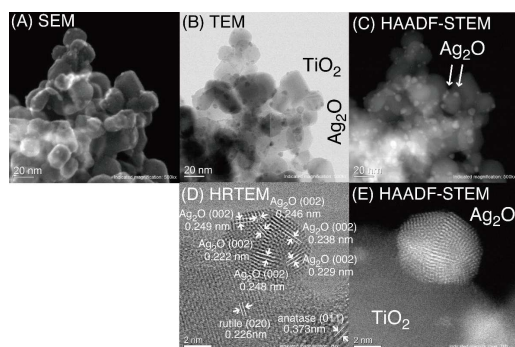


Fig. 2. SEM (A), TEM (B), HR-TEM (D), and HAADF-STEM images (C, E) observed for as-prepared Ag-TiO₂ photocatalyst stored in ambient air.

When the Ag-TiO₂ on the electrode immersed in HCl solution at pH of 2.0 was irradiated by UV-visible light, the yellow color changed to ochre within 10 s (Fig. 1A, Top). For the EXAFS data, the interatomic pair of Ag and Ag became predominant and the distance was 0.287 nm (Fig. 1B-c2, Table S1c). Therefore, all of the outer layer AgCl and a part of inner layer Ag₂O were transformed to metallic yellow Ag⁰ due to the reduction by photogenerated electrons diffused from TiO₂.

In response to the UV-visible irradiation, the photocurrents increased and stabilized within 6–9 min at pH 3.0 (Fig. 3A1). In five light on/off cycles, the photocurrents converged to 11.8–12.7, 17.6–18.8, and 26.0–26.7 μ A using Ag-TiO₂ of 0.33, 1.0, and 3.0 wt%-Ag, respectively, on a photocathode. The converged photocurrent values were plotted as a function of the Ag content in the Ag-TiO₂ photocatalysts (Fig. 3A2), and they increased proportionally to the cube root of the Ag content.

Next, the dependence of photocurrents on the pH of electrolyte

solution was investigated for the PFC comprising TiO₂ and Ag-TiO₂ (3.0 wt% of Ag) at the pH values between 2.0 and 4.0 (Figs. 3B1, 2). Throughout this study, the pH values changed negligibly (within the variation of 0.02) over 5 h. The photocurrents stabilized within 1–11 min of irradiation and converged to 26.0–26.7 μ A at pH 3.0. The current gradually increased from 43.7 to 60.5 μ A in five cycles at pH 2.0 (Fig. 3B1); in contrast, the current gradually decreased from 3.2 to 2.6 μ A at pH 4.0 (B2). The photocurrents quickly decreased to zero over 6 min at pHs of 2.0 and 3.0 when the UV-visible light was off, while the currents decreased more slowly (30–43 min) at pH 4.0. This suggested limited diffusion at lower proton concentrations. The converged PFC photocurrent values were plotted as a function of electrolyte solution proton concentrations (Fig. 3B3). The values increased proportionally to the square root of the proton concentrations.

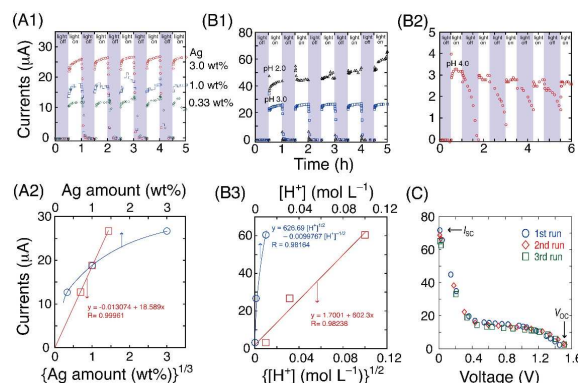


Fig. 3. (A1) The time course of photocurrents of the PFC comprising TiO₂ and Ag-TiO₂ photocatalyst electrodes immersed in HCl solution at pH of 3.0. Circle (○): 3.0 wt% of Ag, square (□): 1.0 wt% of Ag, and diamond (◇): 0.33 wt% of Ag for Ag-TiO₂. (A2) The correlation between converged photocurrents within 5 h and the Ag amount (wt% of Ag) or cube root of the Ag amount and the fits. (B1, 2) The time course of photocurrents in the PFC comprising TiO₂ and Ag-TiO₂ (3.0 wt%-Ag) photocatalyst electrodes, which are immersed in HCl solution at pH of 2.0 (triangle, □), 3.0 (square, □) (B1), and 4.0 (circle, ○) (B2). (B3) The correlation between converged photocurrents within 5 h and the H⁺ concentrations of acid solution in the PFC or the power of square of the H⁺ concentrations. The fits were to linear function (lower x-axis) or to kinetic model equation $i = A[H^+]_c^{1/2} - B[H^+]_c^{-1/2}$ (equation 2, see text; upper x-axis). (C) i - V dependence for PFC comprising TiO₂ and Ag-TiO₂ (3.0 wt%-Ag) immersed in HCl solution at pH of 2.0.

The current (i)-voltage (V) characteristic was also studied for the TiO₂ and Ag-TiO₂ of 3.0 wt%-Ag PFC at pH 2.0 (Fig. 3C). The i value gradually increased as the cell voltage decreased, starting from open circuit voltage (V_{OC} , 1.59 V), which is similar to the i - V dependence for the SCs.²² When the voltage was less than 0.45 V, the current increased linearly from 20 to 74 μ A (short circuit current, I_{SC}). The maximum electric power was 14 μ W (1.1 V \times 13 μ A) among the three runs using the photocatalyst film area of 1.3 cm². As a comparison test, Ag mesh (150 μ m- ϕ , 40 lines in 2.54 cm) was used as electrodes instead of ITO-coated glass. The V_{OC} (0.52 V) and I_{SC} (107 μ A) obtained for PFC using Ag mesh were quite different from that using ITO-coated glass (1.59 V, 74 μ A; Fig. 3C), suggesting the interface between photocatalysts and electrode (In/Sn oxide, Ag) was also critical for the characteristic of PFC.

The i - V characteristic can be explained based on the equivalent SC circuit comprising a diode, a series resistance

(R_{series}), and a shunt resistance (R_{shunt}).²³ The current i can be expressed as follows

$$i = i_{\text{photo}} - i_{\text{diode}} \left[\exp\left(\frac{e(V + iR_{\text{series}})}{nkT}\right) - 1 \right] - \frac{V + iR_{\text{series}}}{R_{\text{shunt}}}, \quad (1)$$

where i_{photo} is photoelectric current, i_{diode} is saturated i of diode, n is a constant for diode, e is elementary charge, k is Boltzmann constant, and T is the temperature of cell. The R_{series} and R_{shunt} values were calculated to be 35 and 5.9 k Ω cm², respectively, based on the tangent lines from V_{OC} and I_{SC} (Fig. 3C). Compared to the general requisite for ideal Si SCs ($R_{\text{series}} < 1 \Omega$ cm², $R_{\text{shunt}} > 1$ k Ω cm²), the resistance in photocatalysts and that at the interface between photocatalysts and electrodes needs to be improved for PFCs to decrease the R_{series} value.

The PFC photocurrents are generated by the balance of photoexcitation and charge recombination in TiO₂ and Ag-TiO₂ photocatalysts, and the reaction rates of water photooxidation and O₂ photoreduction (Scheme 1) analogous to dye-sensitized SCs, in which dye attached to TiO₂ is photooxidized and redox mediator is reduced at the cathode.

The allowed indirect band gap electronic transition²⁴ leads to the separation of electrons and holes in TiO₂. The equilibrium constants of charge separation (K_a and K_c) are assumed in the photoanodic TiO₂ and photocathodic Ag-TiO₂, respectively. The electrons excited to CB for Ag-TiO₂ may be favorably trapped at the Ag sites²⁰ owing to the Schottky barrier (work functions: 4.52–4.74 eV (Ag)²⁵ > 4.13–4.3 eV (TiO₂)^{26,27}). The trap was evidenced by the reduction of Ag^I to Ag⁰ in EXAFS for Ag-TiO₂ immersed in HCl solution and irradiated by UV-visible light (Fig. 1B-c, Table S1c).

The photooxidation over TiO₂ was essentially irreversible in the N₂ flow. The rate and rate constant were denoted as r_{ox} and k_{ox} , respectively. The O₂ photoreduction at Ag-TiO₂ was in equilibrium with the product (water) and the constant is denoted as K_{red} . The forward electron flow rate from TiO₂ to Ag-TiO₂ via the external circuit should be proportional to both the excited electron concentration in TiO₂ and the hole Ag-TiO₂ concentration based on the principle of PFC as shown in Scheme 1. The reverse electron flow rate should be proportional to both the unreacted trapped electron concentration at Ag-TiO₂ and the unreacted hole concentration at TiO₂. Thus, the effective electron flow rate (photocurrent i) is formulated in equation 2. The derivation is shown in equations S1–S4 (ESI[†]).

$$i = k \frac{K_a' (k_{\text{ox}}')^{\frac{1}{4}} (K_c')^{\frac{1}{2}} (K_{\text{red}}')^{\frac{1}{8}}}{(r_{\text{ox}})^{\frac{1}{4}}} \left([\text{O}_2]_c \right)^{\frac{1}{8}} \left([\text{H}^+]_c \right)^{\frac{1}{2}} - k' \frac{(r_{\text{ox}})^{\frac{1}{4}} (K_c)^{\frac{1}{2}}}{(k_{\text{ox}})^{\frac{1}{4}} (K_{\text{red}})^{\frac{1}{8}} \left([\text{O}_2]_c \right)^{\frac{1}{8}} \left([\text{H}^+]_c \right)^{\frac{1}{2}}} \quad (2)$$

where $[\text{O}_2]$ and $[\text{H}^+]$ with a subscript “c” denote the concentrations of O₂ and H⁺ in acidic solution around the cathode, and rate and equilibrium constants with the prime symbol denote the constants multiplied with essentially constant concentrations for predominant species in acidic solution/photocatalysts (See ESI[†] for a detailed definition).

The experimental data fit of pH dependence in equation 2 is presented in Fig. 3B3 (upper x-axis). The second term was negligible in the fit ($i = 626.7 [\text{H}^+]^{1/2} - 0.009977 [\text{H}^+]^{-1/2}$),

demonstrating that the reverse electron flow from Ag to VB of anodic TiO₂ via external circuit was minimal. Moreover, the net photocurrents were essentially proportional to $[\text{H}^+]^{1/2}$ (Fig. 3B3, lower x-axis; the first term of equation 2). In this study, PFC was advantageous for rectifying the electron flow direction owing to the Schottky barrier between TiO₂ and Ag nanoparticles. Moreover, the suppression of reverse reaction at anodic TiO₂ by purging the resultant O₂, analogous to the suppression of dye reduction by electron transfer from CB of TiO₂ to dye in dye-sensitized SC.²² In addition, total current generated in Fig. 3B1 (pH 2.0) corresponded to 4.9 $\mu\text{mol} \cdot \text{e}^-$ versus the Ag amount mounted on cathode was 1.4 μmol . Therefore, major part of forward electron flow to Ag on cathode should be consumed to reduce O₂.

The effects of Ag (electron trap and electron transfer to O₂-derived species) are related to the charge separation equilibrium K_c (or $K_c' = K_c [\text{Ag}^+] [\text{O}^{2-}]$, ESI[†]) that appeared in equation 2. The weight (w) of sphere-like Ag nanoparticles (Fig. 2) is proportional to the cube of average radius ($w = N \frac{4}{3} \pi (r)^3 \rho$, where N : number of Ag nanoparticles, ρ : the density). The effective charges trapped in Ag for photocatalysis should be related to surface area of Ag nanoparticles, $4N\pi(r)^2 = (4N\pi)^{\frac{1}{3}} (3w/\rho)^{\frac{2}{3}}$. The dependence of effective trapped charges on w (2/3) takes into account the square root dependence of the first term in equation 2 on K_c' (2/3 \times 1/2 = 1/3). Thus, the cube root dependence of photocurrents on Ag content (Fig. 3A2) can also be explained.

In the cyclic voltammetry (CV) measurements for Ag-TiO₂ (3.0 wt% of Ag) in HCl aqueous solution of pH 4.0, only the redox reactions of AgCl ($\text{AgCl} + \text{e}^- \rightleftharpoons \text{Ag}^0 + \text{Cl}^-$) and H₂ formation ($2\text{H}^+ + 2\text{e}^- \rightleftharpoons \text{H}_2$) occurred under N₂ in dark (Fig. 4d, Table S2). When the Ag-TiO₂ was irradiated by UV-visible light, the redox reactions of Ag₂O ($\text{Ag}_2\text{O} + 2\text{H}^+ + 2\text{e}^- \rightleftharpoons 2\text{Ag}^0 + \text{H}_2\text{O}$) also occurred (Fig. 4c). Under O₂, the reduction reaction peak from Ag₂O to Ag⁰ at 0.35 V (versus SHE) was more intense, as seen in Fig. 4a, when irradiated by UV-visible light compared to Fig. 4b, which is the reduction peak in the dark. This result is in accordance with the Ag photoreduction as monitored using EXAFS (Figs. 1B-c). If the photoreduction of Ag is coupled with simple oxidation of Ag by O₂ ($4\text{Ag} + \text{O}_2 \rightleftharpoons 2\text{Ag}_2\text{O}$), O₂ photoreduction at the cathode of the PFC can be explained (Fig. 4a, Bottom inset chemical formula). In contrast, no distinct peaks appeared in any of the conditions employed for TiO₂.

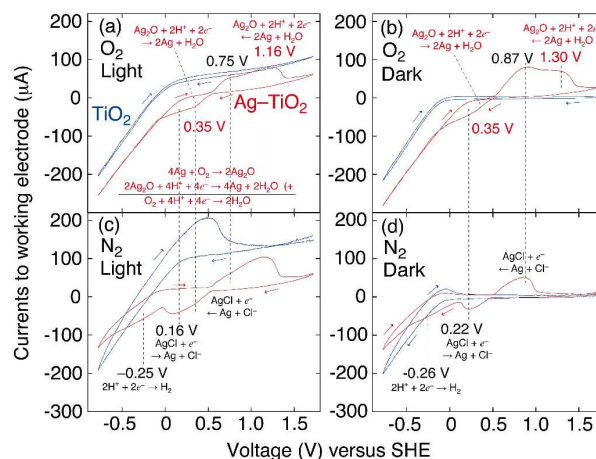


Fig. 4. CV for working electrode of TiO₂ or Ag-TiO₂ (3.0 wt% of Ag) and

counter electrode of glassy carbon in HCl aqueous solution of pH 4.0 in O₂ flow (a, b) or N₂ flow (c, d) under the irradiation by UV-visible light (a, c) or in dark (b, d).

Conclusions

The feasibility of PFCs comprising two photoelectrodes was demonstrated using TiO₂ and Ag-TiO₂ immersed in HCl solution of pH 2, separated by a PCP film. The V_{OC} , I_{SC} , and maximum power were 1.59 V, 74 μ A, and 14 μ W, respectively. TiO₂ photooxidized water under N₂ flow, while Ag-TiO₂ photoreduced O₂. The kinetic model successfully explained the photocurrent dependences on pH values and the amount of Ag. The quantum efficiency was evaluated to be 20% both for photooxidation and photoreduction (ESI†) and that of PFC should be the product (4%). The quantum efficiency needs to be improved by the optimization of photocatalysts on cathode and the thickness, packed density, and the serial resistance for photocatalysts on electrodes.

Notes and references

^a Department of Chemistry, Graduate School of Science, Chiba University, Yayoi 1-33, Inage-ku, Chiba 263-8522, Japan., Fax: +81-43-290-2783; Tel: +81-43-290-3696; E-mail: yizumi@faculty.chiba-u.jp

^b Department of Mechanical Engineering, Graduate School of Engineering, Chiba University, Yayoi 1-33, Inage-ku, Chiba 263-8522, Japan.

^c Department of Chemistry, Faculty of Science, Tokyo University of Science, Kagurazaka 1-3, Shinjuku-ku, Tokyo 163-8601, Japan.

† Electronic Supplementary Information (ESI) available: The derivation of equation 2 for photocurrents of PFC, Experimental methods, EXAFS curve-fit results, CV peak positions, and supplementary EM images. See DOI: 10.1039/b000000x/

‡ The authors are grateful for the financial supports from the Feasibility Study Stage of A-STEP (AS251Z00906L, AS231Z01459C) from the Japan Science and Technology Agency, the Iwatani Naoji Foundation (2011–2012), and the Grant-in-Aid for Scientific Research C (22550117) from MEXT (2010–2012). X-ray absorption experiments were conducted under the approval of the Photon Factory Proposal Review Committee (2013G159).

- 1 N. S. Lewis and D. G. Nocera, *Proc. Natl. Acad. Sci. USA* **2006**, *103*, 15729.
- 2 Y. Izumi, *Coord. Chem. Rev.*, 2013, **257**, 171.
- 3 J. R. Bolton, *Sol. Energy*, 1996, **57**, 37.
- 4 M. Grätzel, *Nature*, 2001, **414**, 338.
- 5 H. A. Gasteiger and N. M. Marković, *Science*, 2009, **324**, 48.
- 6 K. S. Joya, Y. F. Joya, K. Ocaoglu and R. van de Krol, *Angew. Chem. Int. Ed.*, 2013, **52**, 10426.
- 7 X. Chen and S. S. Mao, *Chem. Rev.*, 2007, **107**, 2891.
- 8 N. Serpone, *J. Phys. Chem. B*, 2006, **110**, 24287.
- 9 H. B. Gray, *Nat. Chem.*, 2009, **1**, 7.
- 10 J. K. Hurst, *Science*, 2010, **328**, 315.
- 11 K. Li, Y. Xu, Y. He, C. Yang, Y. Wang and J. Jia, *Environ. Sci. Technol.*, 2013, **47**, 3490.
- 12 P. Lianos, *J. Hazard. Mater.*, 2011, **185**, 575.
- 13 B. D. Alexander, P. J. Kulesza, I. Rutkowska, R. Solarzka and J. Augustynski, *J. Mater. Chem.*, 2008, **18**, 2298.
- 14 K. Ren, Y. X. Gan, T. J. Young, Z. M. Moutassem, L. Zhang, *Composites: B*, 2013, **52**, 292.
- 15 K. Ren, C. A. McConnell, Y. X. Gan, A. A. Afjeh, L. Zhang, *Electrochim. Acta*, 2013, **109**, 162.
- 16 C. Leygraf, M. Hendewerk and G. A. Somorjai, *J. Phys. Chem.*, 1982, **86**, 4484.
- 17 Sayama, K.; Mukasa, K.; Abe, R.; Abe and Y.; Arakawa, H. *Chem. Commun.*, 2001, **35**, 2416.
- 18 K. Fujihara, T. Ohno and M. Matsumura, *J. Chem. Soc. Faraday Trans.*, 1998, **94**, 3705.

- 19 Q. Chen, J. Li, X. Li, K. Huang, B. Zhou, W. Cai and W. Shangguan, *Environ. Sci. Technol.*, 2012, **46**, 11451.
- 20 M. K. Seery, R. George, P. Floris and S. C. Pillai, *J. Photochem. Photobiol. A*, 2007, **189**, 258.
- 21 Predominance of (002) lattices suggested that the Ag₂O particle in Fig. 2D, E was polycrystalline rather than a single crystal.
- 22 A. Y. Anderson, P. R. Barnes, J. R. Durrant and B. C. O'Regan, *J. Phys. Chem. C*, 2011, **115**, 2439.
- 23 K. Bouzidi, M. Chegaar and A. Bouhemadou, *Solar Ener. Mater. Solar Cells*, 2007, **91**, 1647.
- 24 Y. Izumi, T. Itoi, S. Peng, K. Oka and Y. Shibata, *J. Phys. Chem. C*, 2009, **113**, 6706.
- 25 R. C. Weast, Ed-in-chief. *CRC Handbook of Chemistry and Physics* **82**, p.12-130; CRC Press: Boca Raton, USA, 2001.
- 26 A. Imanishi, E. Tsuji and Y. Nakato, *J. Phys. Chem. C*, 2007, **111**, 2128.
- 27 D. O. Scanlon, C. W. Dunnill, J. Buckeridge, S. A. Shevlin, A. J. Lodsail, S. M. Woodley, R. A. Catlow, M. J. Powell, R. G. Palgrave, I. P. Parkin, G. W. Watson, T. W. Keal, P. Sherwood and A. A. Sokol, *Nature Mater.*, 2013, **12**, 798.